

# Optimization of Gutzwiller Wavefunctions in Quantum Monte Carlo

Erik Koch,<sup>(a,b)</sup> Olle Gunnarsson,<sup>(a)</sup> and Richard M. Martin<sup>(b)</sup>

<sup>(a)</sup>Max-Planck-Institut für Festkörperforschung, D-70569 Stuttgart

<sup>(b)</sup>Department of Physics, University of Illinois at Urbana-Champaign, Urbana, IL 61801  
(October 14, 2018)

Gutzwiller functions are popular variational wavefunctions for correlated electrons in Hubbard models. Following the variational principle, we are interested in the Gutzwiller parameters that minimize e.g. the expectation value of the energy. Rewriting the expectation value as a rational function in the Gutzwiller parameters, we find a very efficient way for performing that minimization. The method can be used to optimize general Gutzwiller-type wavefunctions both, in variational and in fixed-node diffusion Monte Carlo.

71.10.Fd, 71.27.+a, 02.70.Lq

## I. INTRODUCTION

The Hubbard Hamiltonian<sup>1-3</sup> is a basic model for studying correlated electrons. Despite its simple form it is very difficult to solve, the main complication arising from the fact that the interaction term is diagonal in real space, while the kinetic energy is simple in momentum space. Except for special cases, namely the one<sup>4</sup> and the infinite-dimensional<sup>5</sup> Hubbard model, no exact solutions are known. For other dimensions we thus have to use approximate methods. The variational method has the advantage of being applicable over the whole range of interaction strength. Naturally, the quality of variational calculations depends critically on the trial function and on our ability to optimize its parameters. A good trial function has to balance the opposing tendencies of the kinetic and the interaction term. Gutzwiller proposed such a wavefunction for the Hubbard model, the Gutzwiller wavefunction (GWF).<sup>1,6,7</sup> It introduces correlations into a Slater determinant by means of a correlation factor that is local in configuration space. Like the Jastrow factor in continuum-space wavefunctions,<sup>8</sup> it works by reducing the weight of configurations with large potential energy. Unfortunately, also the GWF is hard to treat exactly. Again, analytical results have only been obtained in one dimension,<sup>9-12</sup> and in infinite dimensions,<sup>13</sup> where the Gutzwiller approximation (GA) becomes exact.<sup>7,14</sup> For  $1 < d < \infty$  we have to resort to numerical methods like variational Monte Carlo (VMC).<sup>15,16</sup> Another variational method that has been developed recently is fixed-node diffusion Monte Carlo (FNDMC) for Fermions on a lattice.<sup>17,18</sup> Like variational Monte Carlo it uses a trial wavefunction, but the results are much closer to the exact ground state and depend much less on the trial wavefunction. Since these Monte Carlo methods work in configuration space it is straightforward to implement trial functions with more correlation factors. Such generalized Gutzwiller-type wavefunctions<sup>7</sup> that include for example correlations between empty and doubly occupied sites give improvements over the original Gutzwiller wavefunction.<sup>19</sup>

Our goal is to optimize the parameters in Gutzwiller-type wavefunctions in the framework of quantum Monte Carlo calculations. General methods for achieving this are correlated sampling<sup>15,20</sup> or the recently developed stochastic gradient approximation.<sup>21</sup> Exploiting the particular form of Gutzwiller wavefunctions, we find a different approach, which is equivalent to correlated sampling: We observe that expectation values can be rewritten as the quotient of two polynomials (i.e. a rational function) in the Gutzwiller parameters. Estimating the coefficients of these polynomials in a single Monte Carlo run, we can then easily minimize the energy expectation value by finding the minimum of the corresponding rational function. The implementation of this idea in variational Monte Carlo is described in section II. We show how the optimization works in practice and give some applications. In Sec. III the optimization method is adapted to work also in fixed-node diffusion Monte Carlo. This allows us to study the effect of changing the fixed-node constraint in FNDMC. Applications and results for wavefunctions with more parameters are given in Sec. IV.

## II. VARIATIONAL MONTE CARLO

To be specific, we consider the Hubbard model

$$H = -t \sum_{\langle i,j \rangle, \sigma} c_{i,\sigma}^\dagger c_{j,\sigma} + U \sum_i n_{i,\uparrow} n_{i,\downarrow}, \quad (1)$$

where  $c_{i,\sigma}^\dagger$  creates an electron with spin  $\sigma$  on site  $i$  and  $n_{i,\sigma} = c_{i,\sigma}^\dagger c_{i,\sigma}$ . The sum in the kinetic term is over nearest-neighbor pairs, and the hopping matrix element is used as the energy scale, i.e.  $t \equiv 1$ . The interaction term in (1) may also be written as  $UD$ , where  $D = \sum_i n_{i,\uparrow} n_{i,\downarrow}$  is the operator that counts the number of doubly occupied sites. The Gutzwiller wavefunction is then given by

$$|\Psi(g)\rangle = g^D |\Phi_0\rangle, \quad (2)$$

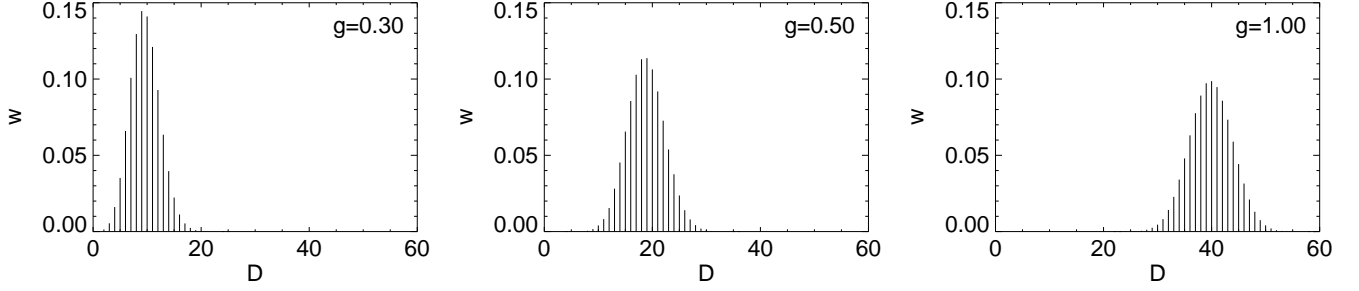


FIG. 1. Weight of configurations with given number  $D$  of double occupancies for the Gutzwiller wavefunction. (The weight  $w(D)$  is defined as the sum of  $\Psi_T^2(R)$  over all configurations  $R$  with  $D$  doubly occupied sites.) Reducing the Gutzwiller factor  $g$  suppresses configurations  $R$  for which the interaction energy  $E_{\text{int}}(R) = U D(R)$  is large — at the expense of increasing the kinetic energy. The results shown are for  $101 + 101$  electrons on a  $16 \times 16$  lattice.

where  $0 \leq g \leq 1$  is the Gutzwiller parameter and  $|\Phi_0\rangle$  is the ground state wavefunction of the non-interacting system ( $U = 0$ ). The Gutzwiller factor builds correlations into the Slater determinant by reducing the weight of configurations with large interaction energy, i.e. large number of doubly occupied sites. This is visualized in Fig. 1.

In the following we briefly review the formalism of variational Monte Carlo for lattice systems and discuss a way to improve the efficiency of the simulation, especially for systems with strong correlation. Then we introduce the method for optimizing the Gutzwiller parameter in a VMC calculation.

### A. Modified Metropolis algorithm

To calculate the energy expectation value for the Gutzwiller wavefunction we have to perform a sum over all configurations  $R$ :

$$E_T = \frac{\langle \Psi_T | H | \Psi_T \rangle}{\langle \Psi_T | \Psi_T \rangle} = \frac{\sum_R E_{\text{loc}}(R) \Psi_T^2(R)}{\sum_R \Psi_T^2(R)}, \quad (3)$$

where we have introduced the local energy for a configuration  $R$ :

$$\begin{aligned} E_{\text{loc}}(R) &= \sum_{R'} \frac{\langle \Psi_T | R' \rangle \langle R' | H | R \rangle}{\langle \Psi_T | R \rangle} \\ &= -t \sum_{R'}' \frac{\Psi_T(R')}{\Psi_T(R)} + U D(R). \end{aligned} \quad (4)$$

The prime in the last equation indicates that the sum is restricted to configurations  $R'$  that are connected with  $R$  by the Hamiltonian, i.e. configurations that can be reached from  $R$  by hopping one electron to a nearest-neighbor site. We call such configurations nearest-neighbors in configuration space.

Since the number of configurations grows combinatorially with system-size, the sums in (3) can in general only be performed for very small systems. For larger problems

we can use Monte Carlo. The idea is to perform a random walk in the space of configurations, with transition probabilities  $p(R \rightarrow R')$  chosen such that the configurations  $R_{\text{VMC}}$  in the random walk have the probability distribution function  $\Psi_T^2(R)$ . Then

$$E_{\text{VMC}} = \frac{\sum_{R_{\text{VMC}}} E_{\text{loc}}(R)}{\sum_{R_{\text{VMC}}} 1} \approx E_T, \quad (5)$$

where the last equality holds within statistical error-bars. The transition probabilities are given by  $p(R \rightarrow R') = 1/N \min[1, \Psi_T^2(R')/\Psi_T^2(R)]$ , with  $N$  being the maximum number of possible transitions.<sup>22</sup> This choice fulfills detailed balance

$$\Psi_T^2(R) p(R \rightarrow R') = \Psi_T^2(R') p(R' \rightarrow R). \quad (6)$$

For ergodicity it is sufficient to consider only transitions between nearest neighboring configurations. The standard prescription is then to propose a transition  $R \rightarrow R'$  with probability  $1/N$  and accept it with probability  $\min[1, \Psi_T^2(R')/\Psi_T^2(R)]$ . This works well for  $U$  not too large. In strongly correlated systems, however, the random walk will stay for long times in configurations with a small number of double occupancies  $D(R)$ , since most of the proposed moves will increase  $D$  and hence be rejected with probability  $\approx 1 - g^{D(R')-D(R)}$ .<sup>23</sup> There is, however, a way to integrate the time the walk stays in a given configuration out. To see how this works, we first observe that for the local energy (4) the ratio of the wavefunctions for all transitions induced by the Hamiltonian have to be calculated. This in turn means that we also know all transition probabilities  $p(R \rightarrow R')$ . We can therefore eliminate any rejection (i. e. make the acceptance ratio equal to one) by proposing moves with probabilities

$$\tilde{p}(R \rightarrow R') = \frac{p(R \rightarrow R')}{\sum_{R'} p(R \rightarrow R')} = \frac{p(R \rightarrow R')}{1 - p_{\text{stay}}(R)}. \quad (7)$$

Checking detailed balance (6) we find that now we are sampling configurations  $R_{\text{VMC}}$  from the probability distribution function  $\Psi_T^2(R) (1 - p_{\text{stay}}(R))$ . To compensate

for this we assign a weight  $w(R) = 1/(1 - p_{\text{stay}}(R))$  to each configuration  $R$ . The energy expectation value is then, within statistical error-bars, given by

$$E_T \approx \frac{\sum_{\bar{R}_{\text{VMC}}} w(\bar{R}) E_{\text{loc}}(\bar{R})}{\sum_{\bar{R}_{\text{VMC}}} w(\bar{R})}. \quad (8)$$

The above method is quite efficient since it ensures that in every Monte Carlo step a new configuration is visited. In other words, the acceptance ratio is one. Instead of staying in a configuration where  $\Psi_T$  is large, this configuration is weighted with the expectation value of the number of times the simple Metropolis algorithm would stay there. This is particularly convenient for simulations of systems with strong correlations: Instead of having to do longer and longer runs as  $U$  is increased, the above method produces, for a fixed number of Monte Carlo steps, results with comparable error-bars.

## B. Optimization

We now turn to the problem of minimizing the energy expectation value (3) as a function of the variational parameters in the trial function. To this end we could simply perform independent VMC calculations for a set of different parameters. It is, however, difficult to compare the energies from independent calculations since each VMC result comes with its own statistical errors. This problem can be avoided with correlated sampling.<sup>15,20</sup> The idea is to use the same random walk in calculating the expectation value for different trial functions. This reduces the relative errors and hence makes it easier to find the minimum.

Let us assume then that we have generated a random walk  $\{R_{\text{VMC}}\}$  for the trial function  $\Psi_T$ . Using the *same* random walk, we can also estimate the energy expectation value (5) for a different trial function  $\tilde{\Psi}_T$ . To do so we have to compensate for the fact that the configurations have the probability distribution  $\Psi_T^2$  instead of  $\tilde{\Psi}_T^2$  by introducing reweighting factors

$$\tilde{E}_T \approx \frac{\sum_{R_{\text{VMC}}} \tilde{E}_{\text{loc}}(R) \tilde{\Psi}_T^2(R)/\Psi_T^2(R)}{\sum_{R_{\text{VMC}}} \tilde{\Psi}_T^2(R)/\Psi_T^2(R)}. \quad (9)$$

Likewise, (8) is reweighted into

$$\tilde{E}_T \approx \frac{\sum_{\bar{R}_{\text{VMC}}} w(\bar{R}) \tilde{E}_{\text{loc}}(\bar{R}) \tilde{\Psi}_T^2(\bar{R})/\Psi_T^2(\bar{R})}{\sum_{\bar{R}_{\text{VMC}}} w(\bar{R}) \tilde{\Psi}_T^2(\bar{R})/\Psi_T^2(\bar{R})}. \quad (10)$$

Also the local energy  $\tilde{E}_{\text{loc}}(R)$  can be rewritten to contain the new trial function only in ratios with the old one. For Gutzwiller functions this implies a drastic simplification. Since they differ only in the Gutzwiller factor, the Slater determinants cancel, leaving only powers  $(\tilde{g}/g)^{D(R)}$ :

$$E_T(\tilde{g}) \approx \frac{\sum_{R_{\text{VMC}}} \tilde{E}_{\text{loc}}(R) (\tilde{g}/g)^{2D(R)}}{\sum_{R_{\text{VMC}}} (\tilde{g}/g)^{2D(R)}} \quad (11)$$

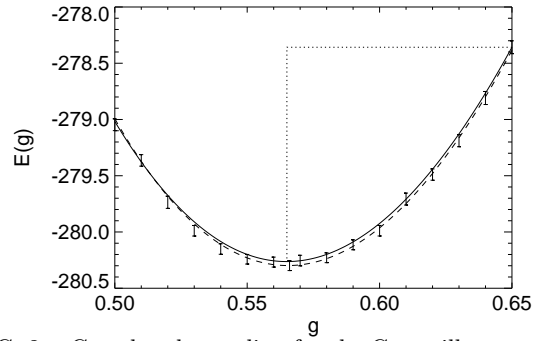


FIG. 2. Correlated sampling for the Gutzwiller parameter  $g$ . The results shown are for 101 + 101 electrons on a  $16 \times 16$  lattice and  $U = 4$ . The full curve shows  $E_T(g)$  calculated using  $g = 0.65$  as Gutzwiller parameter. The predicted minimum  $g_{\text{min}}$  is indicated by the dotted line. The dashed line gives the correlated sampling curve obtained from a calculation with  $g_{\text{min}} = 0.566$ . Both calculations find the same minimum. The error-bars show the results of independent VMC runs for different Gutzwiller parameters. We can clearly see the statistical fluctuations in the results of the separate VMC runs, which, of course, are absent in the correlated sampling curves.

and

$$\tilde{E}_{\text{loc}}(R) = -t \sum_{R'} (\tilde{g}/g)^{(D(R')-D(R))} \frac{\Psi_T(R')}{\Psi_T(R)} + U D(R). \quad (12)$$

Since the number of doubly occupied sites  $D(R)$  for a configuration  $R$  is an *integer*, we can then rearrange the sums in (11) and (12) into polynomials in  $\tilde{g}/g$ . The energy expectation value for any Gutzwiller parameter  $\tilde{g}$  is then given by a rational function in the variable  $\tilde{g}/g$ , where the coefficients only depend on the fixed trial function  $|\Psi(g)\rangle$ .

It is then clear how we proceed to optimize the Gutzwiller parameter in variational Monte Carlo. We first pick a reasonable  $g$  and perform a VMC run for  $|\Psi(g)\rangle$  during which we also estimate the coefficients of the above polynomials. We can then easily calculate  $E_T(\tilde{g})$  by evaluating the rational function in  $\tilde{g}/g$ . Since there are typically only of the order of a few tens non-vanishing coefficients (cf. the distribution of weights shown in Fig. 1), this is a very efficient process.

Figure 2 shows how the method works in practice. Although we deliberately picked a bad starting point we still find the right minimum. The correlated sampling curves even seem to coincide within the statistical errors. This is, however, not true for the whole range of Gutzwiller parameters. When  $\tilde{g}$  differs too much from  $g$ , the method breaks down. To understand this we again turn to Fig. 1. We see that most configurations in a random walk generated with, say,  $g = 0.50$  will have about

20 doubly occupied sites. In the Monte Carlo run we therefore sample the coefficients for  $(\tilde{g}/g)^{2 \times 20}$  best while the statistics for much larger or smaller powers is poor. But it is exactly these poorly sampled coefficients that we need in calculating the energy expectation value for trial functions with  $\tilde{g}$  much different from  $g$ . We can thus use the overlap of the wavefunctions  $\langle \Psi(\tilde{g}) | \Psi(g) \rangle$  as a measure for the reliability of the calculated energy  $E_T(\tilde{g})$ . Like the energy expectation value itself, it can be recast in the form of a rational function, the coefficients of which can be sampled during the VMC run:

$$\begin{aligned} \langle \Psi(\tilde{g}) | \Psi(g) \rangle &= \frac{\sum_R \tilde{\Psi}(R) \Psi(R)}{\sqrt{\sum_R \tilde{\Psi}^2(R) \sum_R \Psi^2(R)}} \\ &= \frac{\sum_{R_{\text{VMC}}} (\tilde{g}/g)^{D(R)}}{\sqrt{\sum_{R_{\text{VMC}}} (\tilde{g}/g)^{2D(R)} \sum_{R_{\text{VMC}}} 1}}. \end{aligned} \quad (13)$$

To get a feeling for the overlap as a function of  $\tilde{g}$  for fixed  $g$ , we can make a rough estimate using the Gutzwiller approximation. Expanding around  $g$  we find that the overlap looks like a Gaussian:  $\exp[-M(\tilde{g}-g)^2/\sigma_0^2]$ , with  $M$  the number of lattice sites. As expected, for  $g$  and  $\tilde{g}$  fixed, the overlap goes to zero exponentially with system size.  $\sigma_0$  is a function of  $g$  and the filling. It generally decreases with  $g$ . This can be understood by looking at Fig. 1 as for small  $g$  the weights are peaked more sharply than for larger Gutzwiller parameters. For half filling the width of the Gaussian is given by  $\sigma_0 = \sqrt{2g} 2(1+g)$ .

The relation between the overlap and the reliability of the expression (11) can best be seen by comparing VMC calculations to exact energies  $E(g)$ . An example is shown in Fig. 3. There we compare the results of VMC calculations for finite Hubbard chains of different size with the exact result for the infinite chain.<sup>9,10</sup> Clearly there are systematic errors in the energy coming from finite size effects in the VMC calculations. But apart from that we find a remarkable agreement between the exact energy  $E(g)$  and the result of the correlated sampling, even for fairly small overlaps. It is also evident from the figure that the overlap for given  $g$  and  $\tilde{g}$  decreases with system size, making optimizations more and more difficult, the larger the system.

We finally mention some straightforward modifications of the scheme we have described above. There are situations where it is more appropriate to minimize the variance in the local energy  $\sigma^2(g)$  rather than the energy  $E(g)$ .<sup>20</sup> Since the variance can also be rewritten in terms of a rational function in  $\tilde{g}/g$ , variance optimization can be implemented in much the same way as the energy minimization that we have described here. Furthermore, it is clear that the method is not restricted to the plain Gutzwiller wavefunction but can be generalized to trial functions with more correlation factors of the type  $r^{c(R)}$ . As long as the correlation function  $c(R)$  is integer-valued on the space of configurations, expectation values for such trial functions can still be rewritten

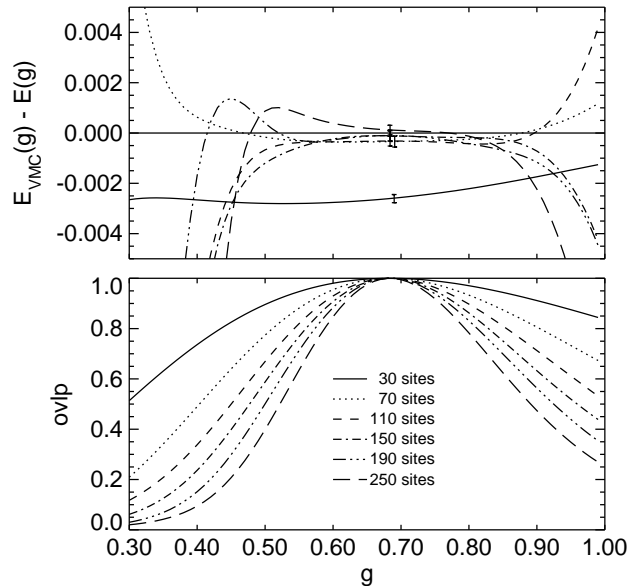


FIG. 3. Comparison of the correlated sampling results for finite Hubbard chains to the exact result for the infinite chain with  $U = 2$ . The energies from the VMC calculations are indicated by the error-bars in the upper figure. The curves give the corresponding results  $E_{\text{VMC}}(g)$  from evaluating expression (11). Clearly there are finite-size errors, especially for the small systems, but apart from that the agreement between the correlated sampling and the exact energy  $E(g)$  for the infinite system is remarkable, even for fairly small overlaps of the trial functions, as can be seen from the lower panel. Eventually, however, when the overlaps become too small (here  $\lesssim 0.4$ ) correlated sampling breaks down.

as rational functions. The only difference to the simpler case described above is that now the rational function is multivariate, reflecting the fact that there is more than one variational parameter.

### III. FIXED-NODE DIFFUSION MONTE CARLO

We now turn to the optimization of the trial function in fixed-node diffusion Monte Carlo (FNDMC). In this method the ground state wavefunction of a given Hamiltonian is projected out from a trial function by repeated application of a suitable operator. For Fermion systems this approach is plagued by the infamous sign-problem, which causes an exponential decay of the signal-to-noise ratio during a simulation. One approach to evade this problem is to use a trial function to fix the nodes of the wavefunctions. This is the fixed-node approximation, which gives variational estimates of the ground state energy as a function of the trial function. Clearly a change in the Jastrow factor, will not change the nodes of the trial function. Hence one would expect the FNDMC results to be independent of such changes. This is actually true for systems in continuum-space.<sup>24,25</sup> For lattice problems, the fixed-node approximation is somewhat

more subtle, and, as it turns out, results also depend on the Gutzwiller parameters.<sup>17,18</sup> Since fixed-node diffusion Monte Carlo, like VMC, is a variational method, it is then important to optimize the Gutzwiller factors. This optimization can again be done using correlated sampling. As in the preceding section, we can rewrite the expression for the energy as a function of the Gutzwiller parameter in terms of a ratio of polynomials. Now, however, the order of the polynomials is not a fixed, small number but increases with the number of Monte Carlo steps. It is therefore not feasible to sample the coefficients directly, as we did above.

We will first briefly review the aspects of fixed-node diffusion Monte Carlo that are important for implementing an optimization scheme for Gutzwiller parameters, then describe how to perform the optimization, and finally show how the method works in practice. For more in-depth discussions and some applications of the FNDMC method see, e.g., Refs. 17,18,26,27.

### A. Fixed-node approximation

Diffusion Monte Carlo<sup>28</sup> allows us, in principle, to sample the true ground state of a Hamiltonian  $H$ . The basic idea is to use a projection operator which has the lowest eigenstate as a fixed point. For a lattice problem, where the spectrum is bounded  $E_n \in [E_0, E_{\max}]$ , the projection is given by

$$|\Psi^{(n+1)}\rangle = [1 - \tau(H - E_0)] |\Psi^{(n)}\rangle, \quad (14)$$

starting with  $|\Psi^{(0)}\rangle = |\Psi_T\rangle$ . If  $\tau < 2/(E_{\max} - E_0)$  and  $|\Psi_T\rangle$  has a non-vanishing overlap with the ground state, the above iteration converges to  $|\Psi_0\rangle$ . There is no time-step error involved. Because of the prohibitively large dimension of the many-body Hilbert space, the matrix-vector product in (14) cannot be done exactly. Instead, we rewrite the equation in configuration space

$$\sum_{R,R'} |R'\rangle \langle R' | \Psi^{(n+1)} \rangle = \sum_{R,R'} |R'\rangle \underbrace{\langle R' | 1 - \tau(H - E_0) | R \rangle}_{\equiv F(R',R)} \langle R | \Psi^{(n)} \rangle \quad (15)$$

and perform the propagation in a stochastic sense:  $\Psi^{(n)}$  is represented by an ensemble of configurations  $R$  with weights  $w(R)$ . The transition matrix element  $F(R', R)$  is rewritten as a transition probability  $p(R \rightarrow R')$  times a normalization factor  $m(R', R)$ . The iteration (15) is then performed stochastically as follows: For each  $R$  we pick a new configuration  $R'$  with probability  $p(R \rightarrow R')$  and multiply its weight by  $m(R', R)$ . Then the new ensemble of configurations  $R'$  with their respective weights represents  $\Psi^{(n+1)}$ . Importance sampling decisively improves the efficiency of this process by replacing  $F(R', R)$  with  $G(R', R) = \langle \Psi_T | R' \rangle F(R', R) / \langle R | \Psi_T \rangle$  so that transitions from configurations where the trial function is

small to configurations with large trial function are enhanced. (15) then takes the form

$$\sum |R'\rangle \langle \Psi_T | R' \rangle \langle R' | \Psi^{(n+1)} \rangle = \sum_{R,R'} |R'\rangle G(R', R) \langle \Psi_T | R \rangle \langle R | \Psi^{(n)} \rangle$$

i.e. the ensemble of configurations now represents the product  $\Psi_T \Psi^{(n)}$ , and the transition probabilities are given by  $p(R \rightarrow R') = |G(R', R)|/m(R', R)$  with  $m(R', R) = \text{sign}[G(R', R)] \sum_{R''} |G(R'', R)|$  absorbing the sign of  $G(R', R)$  and ensuring normalization. After a large number  $n$  of iterations the ground state energy is then given by the mixed estimator

$$E_0^{(n)} = \frac{\langle \Psi_T | H | \Psi^{(n)} \rangle}{\langle \Psi_T | \Psi^{(n)} \rangle} \approx \frac{\sum_R E_{\text{loc}}(R) w^{(n)}(R)}{\sum_R w^{(n)}(R)} \quad (16)$$

with  $w^{(n)}(R_n) = \prod_{i=1}^n m(R_i, R_{i-1})$ . As long as the evolution operator has only non-negative matrix elements  $G(R', R)$ , all weights  $w(R)$  will be positive. If, however,  $G$  has negative matrix elements there will be both configurations with positive and negative weight. Their contributions to the estimator (16) tend to cancel so that eventually the statistical error dominates, rendering the simulation useless. This is the infamous sign problem. A straightforward way to get rid of the sign problem is to remove the offending matrix elements from the Hamiltonian, thus defining a new Hamiltonian  $H_{\text{eff}}$  by

$$\langle R' | H_{\text{eff}} | R \rangle = \begin{cases} 0 & \text{if } G(R', R) < 0 \\ \langle R' | H | R \rangle & \text{else} \end{cases} \quad (17)$$

For each off-diagonal element  $\langle R' | H | R \rangle$  that has been removed, a term is added to the diagonal:

$$\langle R | H_{\text{eff}} | R \rangle = \langle R | H | R \rangle + \sum_{R' \neq R} \Psi_T(R') \langle R' | H | R \rangle / \Psi_T(R).$$

This is the fixed-node approximation for lattice Hamiltonians introduced in Ref. 17.  $H_{\text{eff}}$  is by construction free of the sign problem and variational, i.e.  $E_0^{\text{eff}} \geq E_0$ , and if  $\Psi_T(R')/\Psi_T(R) = \Psi_0(R')/\Psi_0(R)$  for all  $R, R'$  with  $G(R', R) < 0$  the method is exact.

Fixed-node diffusion Monte Carlo for a lattice Hamiltonian thus means that we choose a trial function from which we construct an effective Hamiltonian, the ground state of which is determined by diffusion Monte Carlo. From the equations defining  $H_{\text{eff}}$  we can then understand how the fixed-node results depend on the trial function. Clearly, the off diagonal elements (17) only depend on the sign of the trial function. Since the Gutzwiller term is just a non-negative prefactor, a change of  $g$  will not affect these matrix elements. On the other hand, the diagonal elements  $\langle R | H_{\text{eff}} | R \rangle$  can contain ratios of the trial function on neighboring configurations. In many cases these configurations will differ in the number of doubly occupied sites. Then the Gutzwiller terms will not cancel and the diagonal element of the effective Hamiltonian will depend on the Gutzwiller factor.

## B. Correlated sampling

We are now in the position to describe how we can optimize  $\Psi_T$  or, equivalently, optimize  $H_{\text{eff}}$  using correlated sampling. The idea is again to calculate the energy for a modified Hamiltonian  $\tilde{H}_{\text{eff}}$  using a random walk generated for the original Hamiltonian  $H_{\text{eff}}$ . To find the reweighting factors involved in the calculation we rewrite the mixed estimator

$$\begin{aligned} \tilde{E}_0^{(n)} &= \frac{\langle \tilde{\Psi}_T | \tilde{H}_{\text{eff}} | \tilde{\Psi}^{(n)} \rangle}{\langle \tilde{\Psi}_T | \tilde{\Psi}^{(n)} \rangle} \\ &= \frac{\sum \tilde{E}_{\text{loc}}(R) \prod_{i=1}^n \tilde{G}(R_i, R_{i-1}) \tilde{\Psi}_T^2(R_0)}{\sum \prod_{i=1}^n \tilde{G}(R_i, R_{i-1}) \tilde{\Psi}_T^2(R_0)}. \end{aligned} \quad (18)$$

At first glance it looks like the local energy  $\tilde{E}_{\text{loc}}(R)$  has to be calculated for  $\tilde{H}_{\text{eff}}$ , but keeping track of the sign-flip terms in the diagonal of the effective Hamiltonian we find

$$\tilde{E}_{\text{loc}}(R) = \sum_{R'} \frac{\tilde{\Psi}_T(R')}{\tilde{\Psi}_T(R)} \langle R' | H | R \rangle, \quad (19)$$

which is just the local energy for the original Hamiltonian. Hence, the local energy can be dealt with as in variational Monte Carlo, cf. eqn. (12).

Correlated sampling now means that in the expression (18) for the mixed estimator we do Monte Carlo for the terms  $\prod_{i=1}^n G(R_i, R_{i-1}) \Psi_T^2(R_0)$  instead of  $\prod_{i=1}^n \tilde{G}(R_i, R_{i-1}) \tilde{\Psi}_T^2(R_0)$ . The reweighting factors are thus given by

$$\prod_{i=1}^n \frac{\tilde{G}(R_i, R_{i-1})}{G(R_i, R_{i-1})} \frac{\tilde{\Psi}_T^2(R_0)}{\Psi_T^2(R_0)}. \quad (20)$$

Reintroducing the plain (not importance-sampled) projection operator  $F = 1 - \tau(H - E_0)$ , we can rewrite the reweighting factor for a simple Gutzwiller wavefunction into

$$\prod_{i=1}^n \frac{\tilde{F}(R_i, R_{i-1})}{F(R_i, R_{i-1})} \left( \frac{\tilde{g}}{g} \right)^{D(R_0) + D(R_n)} \quad (21)$$

with the ratio  $\tilde{F}(R', R)/F(R', R) = 1$  for  $R' \neq R$ , and

$$\frac{\tilde{F}(R, R)}{F(R, R)} = \frac{1 - \tau \left[ \sum_{R' \neq R} \frac{\Psi_T(R')}{\Psi_T(R)} \langle R' | H | R \rangle \left( \frac{\tilde{g}}{g} \right)^{\Delta(R', R)} - E_0 \right]}{1 - \tau \left[ \sum_{R' \neq R} \frac{\Psi_T(R')}{\Psi_T(R)} \langle R' | H | R \rangle - E_0 \right]} \quad (22)$$

with  $\Delta(R', R) = D(R') - D(R)$ . This expression is again (as in variational Monte Carlo) a low order polynomial in  $\tilde{g}/g$ . The reweighting factor is, however, a product of

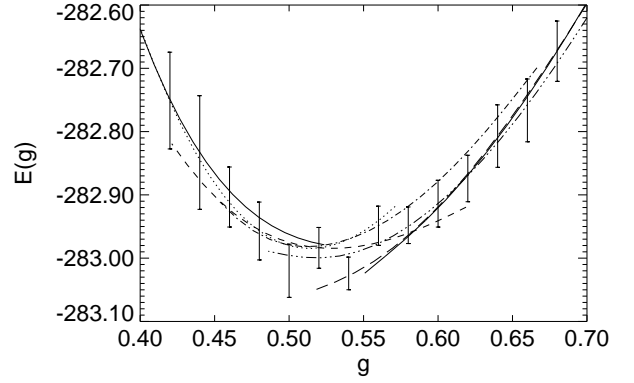


FIG. 4. Correlated sampling for the Gutzwiller parameter  $g$  in fixed-node diffusion Monte Carlo. The results are for the same system as in Fig. 2 (101 + 101 electrons on a  $16 \times 16$  lattice,  $U = 4$ ). The error-bars show the results of independent FNDMC runs for different Gutzwiller parameters. The lines give the results of correlated sampling for trial functions with  $g = 0.44, 0.48, 0.52, 0.56, 0.60, 0.64,$  and  $0.68$ . Note that in fixed-node diffusion Monte Carlo the energy depends much less on the trial function than in variational Monte Carlo: The energy scale is reduced by a factor 5 compared to Fig. 2, although the range of  $g$ -values is expanded by a factor of two.

many such polynomials, therefore the order of the polynomial representing (20) increases with the number  $n$  of Monte Carlo steps. It is therefore not practical to directly estimate the ever increasing number of coefficients for the reweighting factor. But since we still can easily calculate the coefficients for the factors (22) we may use them to evaluate the mixed estimator  $E_0^{(n)}(\tilde{g})$  in each iteration on a set of *predefined* values  $\tilde{g}_i$  of the Gutzwiller parameter.

To see how the method works in practice we look at the same system as in Fig. 2: 101 + 101 electrons on a  $16 \times 16$  lattice, with  $U = 4$ . Figure 4 shows the result of independent FNDMC runs and the corresponding correlated sampling results. We see that our method gives good predictions of the optimum Gutzwiller parameter, even for runs with trial functions that are quite far from optimum. Comparing with variational Monte Carlo, we first notice that the variational energy in FNDMC is substantially lower (by  $\approx 2.5$  eV). We furthermore see that in the fixed-node method there is a pronounced minimum in the energy as a function of the Gutzwiller parameter, although the energy dependence is much smaller than in variational Monte Carlo. This is to be expected since in FNDMC only certain features of the trial function (namely the ratio of the trial function across the nodes) enter the calculation. The situation is, however, different from the fixed-node method for wavefunctions defined in continuum-space, for which changing the Jastrow factor does not change the position of the nodal surfaces and hence also does not systematically change the result of the fixed-node calculation. We finally notice that the optimum Gutzwiller parameter for FNDMC is slightly smaller than that obtained from VMC.

## IV. APPLICATIONS

We have made practical use of the method for optimizing Gutzwiller parameters in our investigations of the doped Fullerides. In this context we work with a Hubbard-like Hamiltonian that describes the conduction electrons in the three-fold degenerate  $t_{1u}$  band:

$$H = \sum_{\langle ij \rangle} \sum_{nn'\sigma} t_{in,jn'} c_{in\sigma}^\dagger c_{jn'\sigma} + U \sum_i \sum_{(n\sigma) < (n'\sigma')} n_{in\sigma} n_{in'\sigma'}, \quad (23)$$

where  $t_{in,jn'}$  is the hopping integral between orbital  $n$  of the molecule on site  $i$  and orbital  $n'$  of molecule  $j$ , and  $U$  is the Coulomb interaction for electrons on the same molecule. For more details on the underlying physics see Refs. 29–33. In the Monte Carlo calculations for the above Hamiltonian, we use trial functions of the Gutzwiller-type

$$|\Psi_T(U_0, g)\rangle = g^D |\Phi(U_0)\rangle, \quad (24)$$

where besides the Gutzwiller parameter  $g$  we also use different types of Slater determinants  $\Phi$ .

### A. More Gutzwiller parameters

To study the static dielectric screening for the  $t_{1u}$  electrons in the doped Fullerides,<sup>32</sup> we determine the response of the charge density to the introduction of a test charge  $q$  placed on molecule  $i_q$ . To describe the test charge the term

$$H_1(q) = qU \sum_{m\sigma} n_{i_q m\sigma} \quad (25)$$

is added to the Hamiltonian (23). In the spirit of the Gutzwiller Ansatz we correspondingly add a second Gutzwiller factor to the wavefunction (24) that reflects the additional interaction term  $qUN_{i_q}$ :

$$|\Psi_T(g, h)\rangle = g^D h^{N_{i_q}} |\Phi\rangle. \quad (26)$$

Finding the best Gutzwiller parameters is now a two dimensional optimization problem. Dealing with polynomials in the two variables  $g$  and  $h$ , the method of correlated sampling works as straightforwardly as described above for the case of a plain Gutzwiller wavefunction. As an example, Fig. 5 shows the result of the optimization, both in variational and in fixed-node diffusion Monte Carlo, for a cluster of 64 C<sub>60</sub> molecules in an fcc arrangement (periodic boundary conditions) resembling K<sub>3</sub>C<sub>60</sub> with a test charge  $q = 1/4$ . In practice we first optimize the parameters in variational Monte Carlo. We then use the optimum VMC parameters as starting points for the optimization in the more time consuming fixed-node diffusion Monte Carlo calculations.

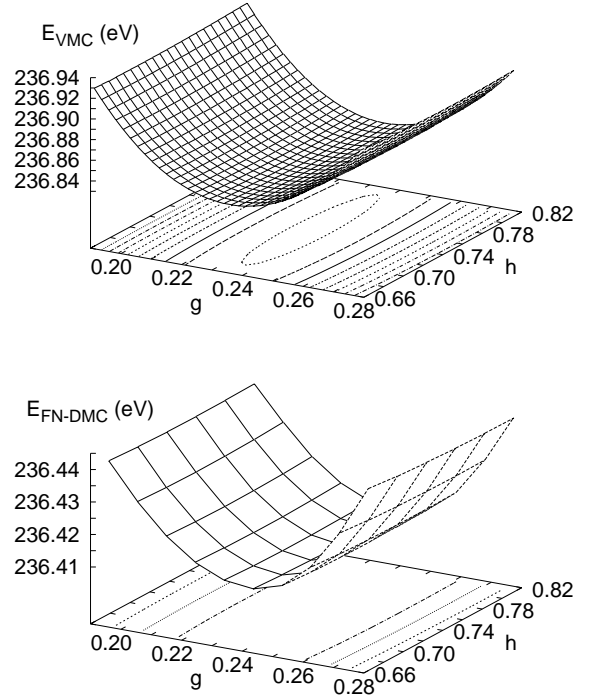


FIG. 5. Correlated sampling for the parameters  $g$  and  $h$  in the generalized Gutzwiller wavefunction  $|\Psi_T\rangle = g^D h^{N_c} |\Phi\rangle$ , cf. eqn. (26) in variational (upper plot) and fixed-node diffusion Monte Carlo (lower plot). The plots show the energy as a function of the Gutzwiller parameters  $g$  and  $h$ , both as surfaces and contours. The calculations were done for an fcc cluster of 64 molecules with 96 + 96 electrons (half-filled  $t_{1u}$ -band), an on-site Hubbard interaction  $U = 1.25$  eV, and a test charge of  $q = 1/4$  (in units of the electron charge).

### B. Variation of Slater determinant

In the traditional Gutzwiller Ansatz, the Slater determinant  $\Phi$  is the ground state wavefunction of the non-interacting Hamiltonian. This is, however, not necessarily the best choice. An alternative would be to use the Slater determinant  $\Phi(U)$  from solving the interacting problem in Hartree-Fock approximation. We can even interpolate between the two extremes by doing a Hartree-Fock calculation with a fictitious Hubbard interaction  $U_0$  to obtain Slater determinants  $\Phi(U_0)$ . Yet another family of Slater determinants  $\Phi(H_{\text{stag}})$  can be obtained from solving the non-interacting Hamiltonian with an added staggered magnetic field, which lets us control the anti-ferromagnetic character of the trial function. Although optimizing parameters in the Slater determinant cannot be done with the method described in the preceding sections, the cheap optimization of the Gutzwiller factors makes it possible to optimize the overall trial function without too much effort.

### 1. Staggered magnetic field

Introducing a staggered magnetic field we can construct Slater determinants by solving the non-interacting Hamiltonian with an added Zeeman term. To be specific, we consider  $K_3C_{60}$  which has a half-filled  $t_{1u}$ -band. Since  $K_3C_{60}$  crystallizes in an fcc lattice, antiferromagnetism is frustrated and the definition of a staggered magnetic field is not unique. We split the fcc lattice into two sublattices  $A$  and  $B$  such that the frustration is minimized. The Zeeman term is then given by

$$H_m = H_{\text{stag}} \sum_i \text{sign}(i) [n_{i\uparrow} - n_{i\downarrow}] \quad (27)$$

with  $\text{sign}(i) = +1$  if  $i \in A$  and  $-1$  if  $i \in B$ . It effectively introduces an on-site energy which, on the same site, has opposite sign for the two spin orientations, and, for the same spin orientation, has opposite sign on the two sublattices. Therefore, hopping to neighboring sites on different sublattices involves an energy cost of twice the Zeeman energy. The staggered magnetic field thus not only induces antiferromagnetic order in the Slater determinant but also serves to localize the electrons. This is reflected in the fact that the optimum Gutzwiller parameter is much larger for Slater determinants constructed from a Hamiltonian with large  $H_{\text{stag}}$  than for paramagnetic Slater determinants. Varying  $H_{\text{stag}}$  then interpolates between paramagnetic/itinerant and antiferromagnetic/localized wavefunctions.

The energy expectation values for such trial functions as calculated in variational Monte Carlo are shown in Fig. 6. It shows  $E_{\text{VMC}}$  as a function of the antiferromagnetic correlation

$$\langle s_i s_{i+1} \rangle = \frac{1}{N} \sum_{\langle ij \rangle} (n_{i\uparrow} - n_{i\downarrow}) (n_{j\uparrow} - n_{j\downarrow}), \quad (28)$$

where the sum is over the  $N$  nearest neighbors.  $\langle s_i s_{i+1} \rangle$  is a monotonous function of  $H_{\text{stag}}$ . For each different value of the Hubbard interaction  $U$  we find a curve with two minima. One minimum is realized for the non-magnetic ( $H_{\text{stag}} = 0$ ) trial function. The energy as a function of  $U$  scales roughly like  $E_{\text{para}} \propto -(1 - U/U_c)^2$ , as predicted by the Gutzwiller approximation. The second minimum is in the antiferromagnetic/localized region and scales roughly like  $E_{\text{AF}} \propto -t^2/U$ , as expected. For small  $U$  the non-magnetic state is more favorable, while for large  $U$  the localized Slater determinant gives lower variational energies. The crossover is at  $U_c \approx 1.50 \text{ eV}$  (dotted line) and resembles a first order phase transition.

### 2. Hartree-Fock

An alternative method for constructing Slater determinants is to use the interacting Hamiltonian with the

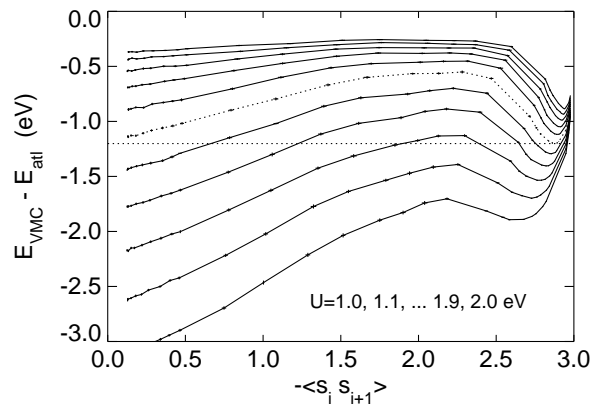


FIG. 6. Variational energy  $E_{\text{VMC}}$  for trial functions with different character. Plotted are the energies (error-bars, lines are to guide the eye) for a Hamiltonian describing  $K_3C_{60}$  (periodic fcc cluster of 32 molecules) with Hubbard interaction  $U = 1.0, 1.1 \dots 1.9, 2.0 \text{ eV}$ . Instead of the total energies  $E_{\text{tot}}$ , we plot the difference of  $E_{\text{tot}}$  and the energy in the atomic limit (each site occupied by three electrons), so that the results for different  $U$  can be readily compared. The trial functions are of the Gutzwiller type. The Slater determinants were determined from diagonalizing the non-interacting Hamiltonian (i.e. setting  $U = 0$ ) with a staggered magnetic field  $H_{\text{stag}}$ . This field gives rise to an antiferromagnetic correlation of neighboring spins, which is plotted on the abscissa. For  $U = 1.5 \text{ eV}$  (dotted curve) the minima in the paramagnetic and the antiferromagnetic region have about the same energy.

physical Hubbard interaction  $U$  replaced by a parameter  $U_0$  and solve it in Hartree-Fock approximation. In practice this is done by simply doing an unrestricted self-consistent calculation for the finite, periodic clusters under consideration, starting from some charge- and spin-density that breaks the symmetry of the Hamiltonian. It is well known that Hartree-Fock favors the antiferromagnetic Mott insulator, predicting a Mott transition at much too small values  $U_c^{\text{HF}}$ . It is therefore not surprising that good trial functions are obtained for values of  $U_0$  considerably smaller than  $U$ . For  $U_0$  close to zero the Slater determinant has metallic character, while for somewhat larger  $U_0$  there is a metal-insulator transition. Figure 7 shows the energy as a function of  $U_0$  for the model of  $K_3C_{60}$ . We find that the results of variational Monte Carlo depend quite strongly on the parameter  $U_0$ . As expected, for fixed Hubbard interaction  $U$  there is a transition from the paramagnetic region for small  $U_0$  to a region where the trial function is antiferromagnetic. In fixed-node diffusion Monte Carlo energies are overall lowered and the dependence on the trial function is much weaker. It seems that here mainly the character (paramagnetic/antiferromagnetic) of the trial function matters. For small  $U$  trial functions with small  $U_0$  give lower energy, while for large  $U$  trial functions with larger  $U_0$  are favorable. The crossover coincides with the Mott transition, which takes place between  $U = 1.50$  and  $1.75 \text{ eV}$ .<sup>30</sup>

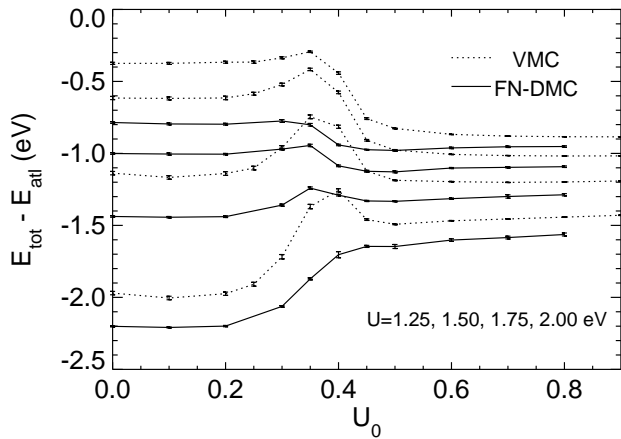


FIG. 7. Dependence of variational (VMC) and fixed-node diffusion Monte Carlo (FN-DMC) on the trial function.  $U_0$  is the Hubbard interaction that was used for the Slater determinant in the Gutzwiller wavefunction  $\Psi_T(R) = g^{D(R)} \Phi(U_0)$ . The results shown here are the energies (relative to the atomic limit) for a Hamiltonian that describes  $K_3C_{60}$  (32 molecules), with  $U$  being varied from 1.25 (lowest curve) to 2.00 eV (highest curve).

## V. SUMMARY

We have presented a convenient and reliable method for optimizing Gutzwiller-type trial functions in Monte Carlo calculations. The method is based on the observation that the expressions for correlated sampling can be rewritten in terms of polynomials in the Gutzwiller parameters. The method can be used both in variational and fixed-node diffusion Monte Carlo. Because of its reliability and speed it makes optimizing Gutzwiller parameters essentially an automatic process. This is especially convenient when dealing with trial functions that have several Gutzwiller parameters as in the example on the dielectric screening in  $K_3C_{60}$ . Given that optimizing the Gutzwiller parameters is quick and easy we can then focus on optimizing the Slater determinant.

## ACKNOWLEDGMENTS

This work has been supported by the Alexander-von-Humboldt-Stiftung under the Feodor-Lynen-Program and the Max-Planck-Forschungspreis, and by the Department of Energy, grant DEFG 02-96ER45439.

- <sup>3</sup> J. Kanamori, Prog.Theor.Phys. **30**, 275 (1963).
- <sup>4</sup> E. Lieb and F. Wu, Phys. Rev. Lett. **20**, 1445 (1968).
- <sup>5</sup> A. Georges, G. Kotliar, W. Krauth, and M. Rozenberg, Rev. Mod. Phys. **68**, 13 (1996).
- <sup>6</sup> M. Gutzwiller, Phys. Rev. **134**, A923 (1964).
- <sup>7</sup> M. Gutzwiller, Phys. Rev. **137**, A1726 (1965).
- <sup>8</sup> R. Jastrow, Phys. Rev. **98**, 1479 (1955).
- <sup>9</sup> W. Metzner and D. Vollhardt, Phys. Rev. Lett. **59**, 121 (1987).
- <sup>10</sup> W. Metzner and D. Vollhardt, Phys. Rev. B **37**, 7382 (1988).
- <sup>11</sup> F. Gebhard and D. Vollhardt, Phys. Rev. Lett. **59**, 1472 (1987).
- <sup>12</sup> F. Gebhard and D. Vollhardt, Phys. Rev. B **38**, 6911 (1988).
- <sup>13</sup> W. Metzner and D. Vollhardt, Phys. Rev. Lett. **62**, 324 (1989).
- <sup>14</sup> D. Vollhardt, Rev. Mod. Phys. **56**, 99 (1984).
- <sup>15</sup> D. Ceperley, G. Chester, and M. Kalos, Phys. Rev. B **16**, 3081 (1977).
- <sup>16</sup> P. Horsch and T. Kaplan, J. Phys. C **16**, L1203 (1983).
- <sup>17</sup> D. ten Haaf, H. van Bommel, J. van Leeuwen, and W. van Saarloos, Phys. Rev. Lett. **72**, 2442 (1994).
- <sup>18</sup> D. ten Haaf, H. van Bommel, J. van Leeuwen, W. van Saarloos, and D. Ceperley, Phys. Rev. B **51**, 13039 (1995).
- <sup>19</sup> T. Kaplan, P. Horsch, and P. Fulde, Phys. Rev. Lett. **49**, 889 (1982).
- <sup>20</sup> C. Umrigar, K. Wilson, and J. Wilkins, Phys. Rev. Lett. **60**, 1719 (1988).
- <sup>21</sup> A. Harju, B. Barbiellini, S. Siljamaki, R. Nieminen, and G. Ortiz, Phys. Rev. Lett. **79**, 1173 (1997).
- <sup>22</sup> This complication arises from the fact that the number of transitions allowed by the Pauli principle in general is different for different configurations. This issue is discussed in Ref. 16.
- <sup>23</sup> H. Yokoyama and H. Shiba, J. Phys. Soc. Jpn. **56**, 1490 (1987).
- <sup>24</sup> D. Ceperley and B. Alder, Phys. Rev. Lett. **45**, 566 (1980).
- <sup>25</sup> D. Ceperley and B. Alder, Science **231**, 555 (1986).
- <sup>26</sup> M. Calandra Buonaura and S. Sorella, Phys. Rev. B **57**, 11446 (1998).
- <sup>27</sup> G. Bachelet and A. Cosentini, in *Quantum Monte Carlo Methods in Physics and Chemistry, NATO-ASI*, edited by C. Umrigar and M. Nightingale (Kluwer, Dordrecht, 1998).
- <sup>28</sup> N. Trivedi and D. Ceperley, Phys. Rev. B **41**, 4552 (1990).
- <sup>29</sup> O. Gunnarsson, Rev. Mod. Phys. **69**, 575 (1997).
- <sup>30</sup> O. Gunnarsson, E. Koch, and R. Martin, Phys. Rev. B **54**, R11026 (1996).
- <sup>31</sup> F. Aryasetiawan, O. Gunnarsson, E. Koch, and R. Martin, Phys. Rev. B **55**, R10165 (1997).
- <sup>32</sup> E. Koch, O. Gunnarsson, and R. Martin, in *Electronic Properties of Novel Materials*, edited by H. Kuzmany, J. Fink, M. Mehring, and S. Roth (American Institute of Physics, New York, 1998).
- <sup>33</sup> E. Koch, O. Gunnarsson, and R. Martin, in *Quantum Monte Carlo Methods in Physics and Chemistry, NATO-ASI*, edited by C. Umrigar and M. Nightingale (Kluwer, Dordrecht, 1998).

<sup>1</sup> M. Gutzwiller, Phys. Rev. Lett. **10**, 159 (1963).

<sup>2</sup> J. Hubbard, Proc.R.Soc.London, Sect.A **276**, 238 (1963).